

## Laser-Target Interaction with Induced Spatial Incoherence

S. P. Obenshain, J. Grun, M. J. Herbst, K. J. Kearney, C. K. Manka, E. A. McLean, A. N. Mostovych, J. A. Stamper, R. R. Whitlock, S. E. Bodner, J. H. Gardner, and R. H. Lehmburg

*U. S. Naval Research Laboratory, Washington, D.C. 20375*

(Received 28 March 1986)

An optical technique called induced spatial incoherence can produce the highly uniform laser beams required for direct-illumination laser fusion. Here we present experimental data on laser-plasma interactions showing that the technique, when used in combination with short laser wavelength, also improves the coupling physics.

PACS numbers: 52.40.Nk

High-gain laser fusion requires a highly symmetric pellet implosion, with pressure nonuniformities around the sphere of no more than a few percent.<sup>1</sup> For the case of directly illuminated pellets, one seeks to obtain such symmetry by the combination of uniform laser illumination and thermal smoothing in the blowoff plasma. Little thermal smoothing is expected for the short laser wavelengths that are required for good laser-target coupling.<sup>2</sup> Complex, high-power lasers, by themselves, do not have sufficient beam quality to achieve the required symmetry. Therefore several beam-smoothing techniques have been proposed which allow uniform illumination of targets with imperfect lasers.<sup>3-6</sup> All of these techniques change the beam sufficiently that one must be concerned about accompanying changes in high-power laser-plasma interactions. Laser-target experiments using the random-phase mask technique were described in a recent paper.<sup>3</sup> Here we present experimental results obtained with the technique of induced spatial incoherence (ISI).<sup>4</sup> When ISI is used in combination with short laser wavelength, the laser-plasma coupling physics improves over that obtained with an ordinary laser beam. Furthermore, the coupling physics obtained with ISI may be superior to that obtained with the random-phase mask technique.

Figure 1 shows our experimental setup to implement ISI. A broad-bandwidth laser beam is divided into numerous independent beamlets by an orthogonal pair of reflecting, echelonlike mirrors. The echelons impose time delays between the beamlets where the incremental delays are longer than the laser coherence time  $\tau_c = 1/\Delta\nu$ . The beamlets are then overlapped onto the target by a lens. The overlapped beamlets form an instantaneous interference pattern. However, if one averages over times long compared to the coherence time, the interference pattern disappears and the focal pattern converges to a smooth profile. This temporal smoothing distinguishes ISI from the random-phase mask technique where the interference pattern from overlapped beamlets remains frozen in the focal distribution.

An important concern is whether a fusion target would react to ISI's instantaneous irradiation nonuniformity. Presently available high-power lasers can attain coherence times as short as 1 psec. Time scales for gross hydrodynamic motion of the pellet shell are of the order of hundreds of picoseconds. Thus, viewed hydrodynamically, the fusion should only respond to the time-averaged smooth profile obtained with ISI. However, laser-plasma instabilities, such as parametric instabilities and filamentation, respond much faster than the hydrodynamics and may be enhanced by the instantaneous beam nonuniformity. The bandwidth utilized with ISI might also affect the laser-plasma interaction.

Our laser-plasma coupling experiments were performed with the following variations: narrow and

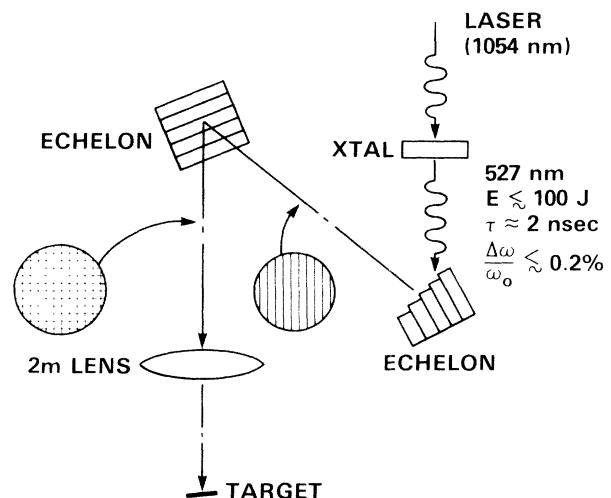


FIG. 1. The experimental arrangement for studying laser-target interaction with ISI. Reflective delays increase by 2 psec per step for the first (vertical) echelon and 40 psec per step for the second (horizontal) echelon. Reflection from the pair of echelons divides the 19-cm-diameter laser beam into  $1 \times 1\text{-cm}^2$  beamlets, each of which has a slightly different optical delay. Smooth focal distributions are obtained when the laser coherence time is shorter than 2 psec.

broad laser bandwidth; short (527-nm) and long (1054-nm) laser wavelength; with and without ISI echelons. We found that all of these factors affected the interaction physics. The best coupling for the fusion application occurred with the combination of broad bandwidth, ISI echelons, and short laser wavelength.

Theory has predicted that wide laser bandwidth would suppress deleterious parametric instabilities that occur with high-power laser-plasma interaction.<sup>7-9</sup> These expectations were only partially realized in broadband laser-matter interaction experiments conducted by Yamanaka *et al.*<sup>10</sup> and Obenschain *et al.*<sup>11</sup> using a relatively long-wavelength laser (1054 nm) and bandwidths below 1%. In both experiments, laser absorption increased with bandwidth, probably as a result of suppression of stimulated scattering. However, both experiments also showed that hot-electron generation increased with bandwidth. A correlation of hard x rays with increased second-harmonic ( $2\omega_0$ ) emission indicated that some phenomenon occurring at near-critical density was probably responsible for this effect. The bandwidths involved were comparable to the expected ion-acoustic frequency for the parametric decay instability, and the bandwidth may have been seeding this instability.<sup>12</sup>

Using similar bandwidths and the same 1054-nm wavelength, we investigated the interaction physics with the addition of ISI echelons. The results were similar to those obtained without the echelons. With sufficient bandwidth for the ISI to work with our echelons (0.15%), we observed increased absorption and increased hot-electron generation. Hard x rays were again correlated with  $2\omega_0$  emission. In contrast,  $\frac{3}{2}\omega_0$  emission decreased with bandwidth, which implied that quarter-critical instability was being suppressed. Details of these spectroscopic measurements will be presented elsewhere.

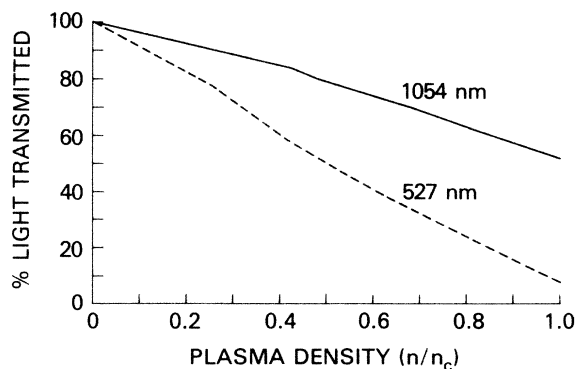


FIG. 2. Calculated transmission of laser light through the blowoff plasma with a 300- $\mu\text{m}$  focal diameter and  $I \approx 10^{14}$  W/cm<sup>2</sup>. More light is transmitted to critical density with 1054-nm light than with 527-nm light.

The experiments utilizing a 1054-nm wavelength laser imply that laser bandwidth suppresses underdense plasma instability, while it enhances some critical-region instability that produces hot electrons. If this is so, then one can solve the hot-electron problem by using a shorter laser wavelength, so that the increased collisional absorption prevents laser light from reaching the critical density region. Figure 2 shows a computer calculation<sup>13</sup> of laser light transmitted as a function of plasma density for the case of 1054- and 527-nm laser wavelengths and intensities near  $10^{14}$  W/cm<sup>2</sup>. Much less light reaches the critical region with the shorter laser wavelength because the blowoff plasma is cooler, denser, and thus more absorbing. With this in mind, we repeated the experiments at 527 nm.

Broadband green light was obtained by frequency doubling of a broadband 1054-nm beam produced by the Pharos III Nd-glass laser (see Fig. 1). The bandwidth of the green light was monitored by a spectrograph. Laser energies on target of up to 100 J and trapezoidal-shaped pulses of 2 nsec FWHM were employed. The echelons divided the laser beam into an array of several hundred ( $1 \times 1$ )-cm<sup>2</sup> beamlets with minimum differential delays of 2 psec. The beamlets were focused with a 2-m lens onto thick polystyrene targets. Figures 3(a) and 3(b) show typical (time-averaged) focal distributions obtained with use of this setup with broad ( $\tau_c = 1$  psec) and narrower ( $\tau_c = 8$  psec) bandwidths. With the shorter coherence time, the focal distribution was very smooth. The relatively flat top on the distribution was obtained by slightly tilt-

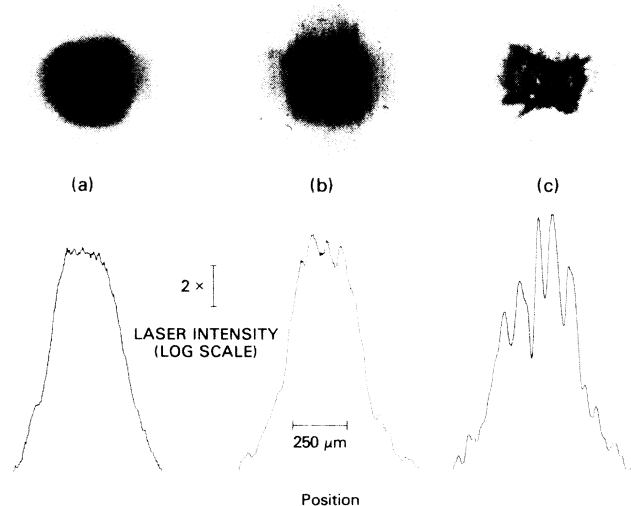


FIG. 3. Photographic and film densitometry measurements of the focal distributions obtained (a) with the ISI echelons and broad laser bandwidth ( $\tau_c = 1$  psec), (b) with echelons and narrower laser bandwidth ( $\tau_c = 8$  psec), and (c) without the echelons. Film grain is contributing to the small-amplitude nonuniformity observed in (a).

ing every other mirror of the echelons to produce four partially overlapping sets of beamlets at the target. With longer coherence time (8 psec), a portion of the overlapped beamlets interfere and produce modulations in the focal distribution. Finally, a focal distribution with the same laser beam but without the ISI echelons is shown in Fig. 3(c). The focal diameter was adjusted by moving the lens to match the diameter obtained with ISI. The focused light then shows large-amplitude modulations due to laser imperfections.

Laser-coupling experiments at 527 nm were conducted with intensities of  $10^{13}$  to  $10^{14}$  W/cm<sup>2</sup>. Arrays of detectors monitored the hard x-ray spectra, scattered light, and harmonic emission. In particular, the continuum x-ray spectra were detected using an array of *p-i-n* diodes and scintillator photomultipliers with *K*-edge filters.<sup>14</sup> Figures 4(a) and 4(b) show the hard x-ray emission near 25 keV and the  $2\omega_0$  emission plotted as a function of irradiance. For the data with ISI, the irradiance is the average across the flat portion of the focal distributions. Without ISI, the irradiance is the average within the focal contour enclosing 80% of the energy. With the echelons in place, the hard x rays and  $2\omega_0$  emission both decrease with the larger bandwidth. These 527-nm results reverse the deleterious effects seen at increased bandwidth with 1054-nm illumination. However, the beneficial effects observed in the 1054-nm experiments remained. Backscatter and  $\frac{3}{2}\omega_0$  emission decreased with the larger bandwidth.

With the echelons in place and with short laser wavelength, the interaction physics improves with increased bandwidth. Moreover, ISI (echelons plus

broad bandwidth) improves the interaction physics over that obtained with an ordinary beam. The hard x-ray emission plotted in Fig. 4(a) is much higher for the cases with no ISI echelons. Figure 4(c) shows the hard x-ray spectra with and without ISI at intensities near  $7 \times 10^{13}$  W/cm<sup>2</sup>. When ISI was used, the intensity of hard x rays at energies above 25 keV was reduced by at least 2 orders of magnitude to levels below the noise in our detectors. These measurements imply that the hot-electron temperature was reduced from about 20 keV without ISI to below 4 keV with ISI. In addition, ISI reduced the backscatter by a factor of 5,  $2\omega_0$  by a factor of 50, and  $\frac{3}{2}\omega_0$  by a factor of 100 over that obtained without the echelons.

The following model of the interaction appears to fit our results. (1) The smooth beam obtained with ISI echelons and broad bandwidth suppresses effects of hot spots, preventing for example the seeding of the self-focusing instability. (2) The combination of this smooth beam with the stabilizing effect of the bandwidth itself suppresses underdense parametric instabilities. (3) The shorter laser wavelength prevents light from reaching critical density and thereby suppresses any enhancement of hot electrons with bandwidth.

The results imply that coherence times of 1 psec are short enough in the present experiment to prevent underdense instabilities from reacting to the "instantaneous" hot spots that occur with ISI. Our computer calculations indicate that the hot spots must persist for about 10 psec before there is sufficient local heating of the plasma to increase the transmissivity to critical density. With narrower bandwidth and the echelons in

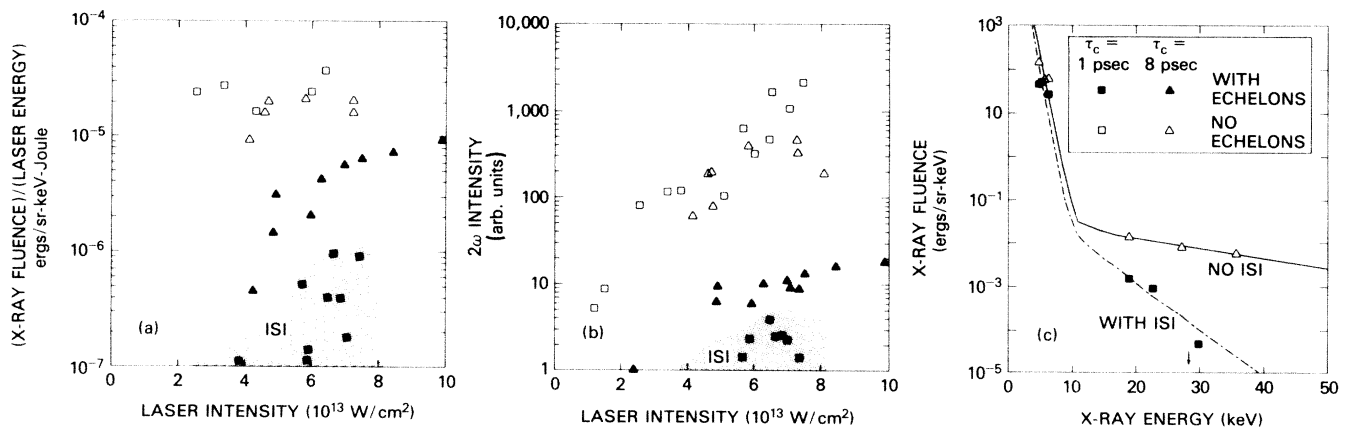


FIG. 4. (a) X-ray emission near 25 keV as a function of laser intensity. (b) Second harmonic emission (263 nm) as a function of laser intensity. The measurements in both (a) and (b) were taken at an angle of  $45^\circ$  with respect to the target normal. (c) Hard x-ray spectra with and without ISI for  $I \approx 7 \times 10^{13}$  W/cm<sup>2</sup>. The lines are bi-Maxwellian fits to the data. The cold component is about 550 eV with or without ISI. The hot component fits 20 keV without ISI and 4 keV with ISI. The signals from the hard x-ray fluence ( $\geq 25$  keV) with ISI were small enough to be masked by noise in our detecting system. The hard x-ray fluence with ISI shown in (a) and (c) is calculated from the sum of signal and noise and should be regarded as upper bounds on the actual fluence.

place, two things happen to the focal distribution which could contribute to the observed deterioration in the interaction physics. First, the "instantaneous" nonuniformity due to interference among all beamlets persists for a longer time and thus is more likely to drive parametric instabilities and self-focusing. Second, the time-averaged residual focal nonuniformity [Fig. 3(b)] could also contribute to instability growth. With still narrower bandwidths, the focal distribution obtained with the ISI echelons would converge on that obtained with the random-phase mask technique, where there are large-amplitude, short-scale-length intensity nonuniformities due to interference among all the overlapped beamlets. The improved coupling we observed with increased bandwidth implies that it is advantageous to eliminate this illumination nonuniformity. Without the ISI echelons, the interaction physics deteriorated markedly. An interesting, but perhaps unattainable, experiment would be to compare the ISI results to those obtained with a nearly perfect narrow-bandwidth laser beam to see if the instability suppression is solely due to the elimination of hot spots in the focused laser.

We extended our investigation of ISI to higher intensity ( $2 \times 10^{14}$  W/cm<sup>2</sup>) by exactly overlapping the beamlets to obtain a tighter, more peaked focus. With the higher laser intensity, the hard x rays rose above threshold of our detectors, but, most importantly, the trend of reduced hard x-ray emission with increased bandwidth remained. Eventually, at very high intensities, we would expect the laser light to bleach through the blowoff plasma and perhaps again excite a critical density instability. This effect could presumably be postponed by using a still shorter laser wavelength than employed here.

Our experiments have reached values of  $I\lambda^2$  appropriate to some high-gain pellet designs. But high-gain targets will involve much larger laser-plasma interaction volumes where the Raman instability can dominate hot-electron generation. Studies of this regime with ISI is an interesting avenue for future research.

In conclusion, with short laser wavelength, the ISI technique improves the interaction physics in addition

to producing a very uniform focal profile. It may be that we are addressing a new physics regime with ISI where, for the first time, the high-power interaction physics is not being dominated by the effects of hot spots in the focal pattern.

We wish to acknowledge useful discussions with F. C. Young, B. H. Ripin, A. J. Schmitt, and B. Afeyan. Mr. Robert A. Hunsicker of Commonwealth Technology collaborated extensively in the design of the echelons. We thank M. Pronko, N. E. Nocerino, and J. P. Bone for their efforts in the design and construction of the laser system used in these experiments. This research was supported by the U. S. Department of Energy.

<sup>1</sup>S. E. Bodner, *J. Fusion Energy* **1**, 221 (1981).

<sup>2</sup>J. H. Gardner and S. E. Bodner, *Phys. Rev. Lett.* **47**, 1137 (1981).

<sup>3</sup>Y. Kato, K. Mima, M. Miyanaka, S. Arinaga, Y. Kitagawa, M. Nakatsuka, and C. Yamanaka, *Phys. Rev. Lett.* **53**, 1057 (1984).

<sup>4</sup>R. H. Lehmburg and S. P. Obenschain, *Opt. Commun.* **46**, 27 (1983).

<sup>5</sup>Ximing Deng, Xiangchun Liang, Zezun Chen, Wenyan Yu, and Renyong Ma, *Chin. J. Lasers* **12**, 257 (1985).

<sup>6</sup>V. V. Alexandrov and V. Mejevov, in *Proceedings of the Seventeenth European Conference on Laser Interaction with Matter*, Rome, 1985 (unpublished).

<sup>7</sup>J. J. Thomson, *Nucl. Fusion* **15**, 237 (1975).

<sup>8</sup>G. Laval *et al.*, *Phys. Fluids* **20**, 2049 (1977).

<sup>9</sup>Kent Estabrook *et al.*, *Phys. Rev. Lett.* **46**, 724 (1981).

<sup>10</sup>C. Yamanaka, T. Yamanaka, T. Sasaki, J. Mizui, and H. B. Kang, *Phys. Rev. Lett.* **32**, 1038 (1974).

<sup>11</sup>S. P. Obenschain *et al.*, in *Thirteenth International Quantum Electronics Conference: Digest of Technical Papers*, *J. Opt. Soc. Am. B* **1**, No. 3 (1984).

<sup>12</sup>D. Arnush *et al.*, *Phys. Fluids* **16**, 2270 (1973).

<sup>13</sup>The computer calculations were made using a 2D hydrocode developed by J. Boris and M. E. Emery at the Naval Research Laboratory.

<sup>14</sup>F. C. Young, in *Naval Research Laboratory Memorandum Report No. 3591*, edited by S. E. Bodner, 1977 (unpublished), pp. 41ff.

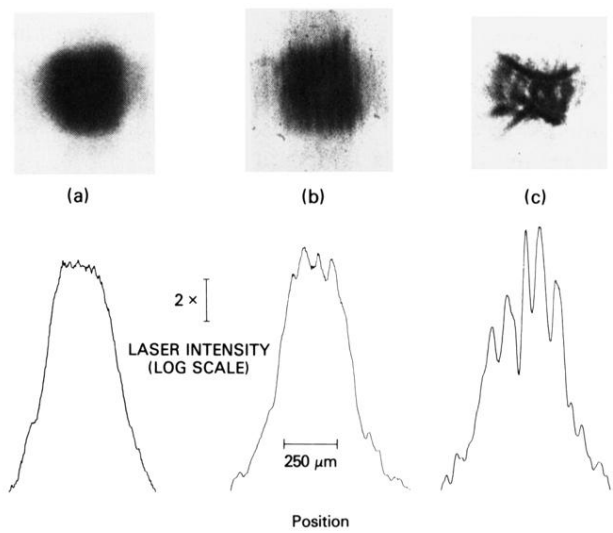


FIG. 3. Photographic and film densitometry measurements of the focal distributions obtained (a) with the ISI echelons and broad laser bandwidth ( $\tau_c = 1$  psec), (b) with echelons and narrower laser bandwidth ( $\tau_c = 8$  psec), and (c) without the echelons. Film grain is contributing to the small-amplitude nonuniformity observed in (a).

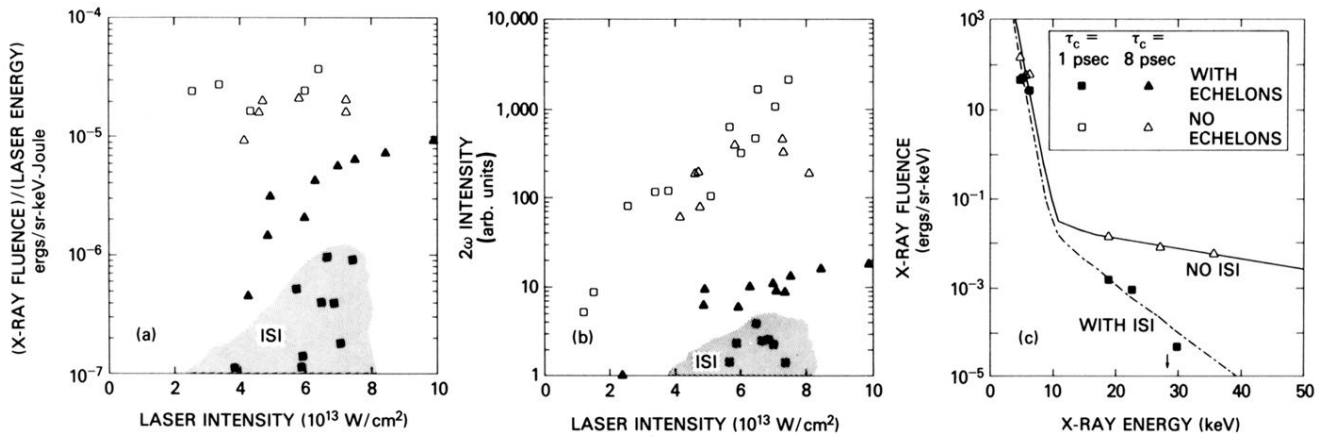


FIG. 4. (a) X-ray emission near 25 keV as a function of laser intensity. (b) Second harmonic emission (263 nm) as a function of laser intensity. The measurements in both (a) and (b) were taken at an angle of 45° with respect to the target normal. (c) Hard x-ray spectra with and without ISI for  $I \approx 7 \times 10^{13}$  W/cm<sup>2</sup>. The lines are bi-Maxwellian fits to the data. The cold component is about 550 eV with or without ISI. The hot component fits 20 keV without ISI and 4 keV with ISI. The signals from the hard x-ray fluence ( $\geq 25$  keV) with ISI were small enough to be masked by noise in our detecting system. The hard x-ray fluence with ISI shown in (a) and (c) is calculated from the sum of signal and noise and should be regarded as upper bounds on the actual fluence.